

Title	Mechanism for the atomic layer deposition of copper using diethylzinc as the reducing agent – a density functional theory study using gas phase molecules as a model
Authors	Dey, Gangotri; Elliott, Simon D.
Publication date	2012-08-14
Original Citation	Dey, G and Elliott, S. D. (2012). Mechanism for the atomic layer deposition of copper using diethylzinc as the reducing agent – a Density Functional Theory study using gas phase molecules as a model. Journal of Physical Chemistry A, 116 (35), pp 8893–8901. DOI: 10.1021/jp304460z
Type of publication	Article (peer-reviewed)
Link to publisher's version	<a href="http://pubs.acs.org/doi/abs/10.1021/jp304460z">http://pubs.acs.org/doi/abs/10.1021/jp304460z</a> - 10.1021/jp304460z
Rights	© 2012, American Chemical Society. This document is the Accepted Manuscript version of a Published Work that appeared in final form in the Journal of Physical Chemistry A, copyright © American Chemical Society after peer review and technical editing by the publisher. To access the final edited and published work see <a href="http://pubs.acs.org/doi/abs/10.1021/jp304460z">http://pubs.acs.org/doi/abs/10.1021/jp304460z</a>
Download date	2024-03-29 04:34:19
Item downloaded from	<a href="https://hdl.handle.net/10468/1054">https://hdl.handle.net/10468/1054</a>



# UCC

**University College Cork, Ireland**  
Coláiste na hOllscoile Corcaigh

# Mechanism for the atomic layer deposition of copper using diethylzinc as the reducing agent – a Density Functional Theory study using gas phase molecules as a model

*Gangotri Dey, Simon D. Elliott*

Tyndall National Institute, University College Cork, Dyke Parade, Lee Maltings, Cork, Ireland

gangotri.dey@tyndall.ie, [simon.elliott@tyndall.ie](mailto:simon.elliott@tyndall.ie)

We present theoretical studies based on first principles density functional theory calculations for the possible gas phase mechanism of the atomic layer deposition (ALD) of copper by transmetallation from common precursors like  $\text{Cu}(\text{acac})_2$ ,  $\text{Cu}(\text{hfac})_2$ ,  $\text{Cu}(\text{PyrIm}^{\text{R}})_2$   $\text{R}=\text{iPr}$ ,  $\text{R}=\text{Et}$ ,  $\text{Cu}(\text{dmap})_2$  and  $\text{CuCl}_2$  where diethylzinc acts as the reducing agent. The effect on geometry and reactivity of the precursors due to the differences in electronegativity, steric hindrance and conjugation present in the ligands was observed. Three reaction types – disproportionation, ligand exchange and reductive elimination - have been considered that together comprise the mechanism for the formation of copper in its metallic state starting from the precursors. A parallel pathway for the formation of zinc in its metallic form has also been considered. The model Cu(I) molecule  $\text{Cu}_2\text{L}_2$  has been studied, as Cu(I) intermediates at the surface play an important role in copper deposition. Through our study we see that accumulation of an  $\text{LZnEt}$  intermediate will result in zinc contamination either by the formation

of  $\text{Zn}_2\text{L}_2$  or metallic zinc. Ligand exchange between  $\text{Cu(II)}$  and  $\text{Zn(II)}$  should go via a  $\text{Cu(I)}$  intermediate, as otherwise it will lead to a stable copper molecule rather than copper metal. Volatile  $\text{ZnL}_2$  will favor the ALD reaction as it will carry the reaction forward.

Keywords: copper atomic layer deposition, diethylzinc, reducing agent, density functional theory.

## Introduction

The modern electronics industry has an urgent need to incorporate a conformal nanometer-thin layer of copper to be used as a seed layer for the subsequent electrodeposition of copper in interconnects. The International Technology Roadmap for Semiconductors describes this as an urgent challenge<sup>1</sup>. Currently, the seed layer is deposited using ionized physical vapor deposition (iPVD). However, iPVD cannot meet the requirements of scaling down of the device size, as this will require the aspect ratio of interconnect to increase. At dimensions below 20 nm, iPVD produces defective nonconformal layers which might result in overhanging and discontinuity of the copper film. The voids can only be filled after electrodeposition, which lowers the reliability of interconnect due to fast electromigration pathways on the void surfaces.

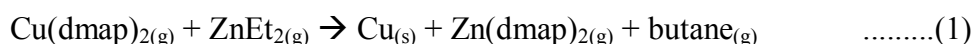
Atomic layer deposition (ALD) is a good alternative to form a thin conformal layer. This process is used in the semiconductor industry to deposit high-k dielectric materials. Although ALD has been explored for oxides, nitrides and sulfides, it is proving difficult to achieve the ALD of many metals, such as copper. The difficulty lies in finding a proper co-reagent for metal ALD. One of the specific difficulties faced for copper is the nucleation mode that results in the formation of islands, rather than a continuous film. Hence we are seeking low temperature ALD so as to avoid aggregation. In addition to that the reducing or oxidizing nature of the co-reagent may limit its use on sensitive substrates.

The distinguishing characteristic of ALD is the separate and alternate pulsing into the reactor of two or more gaseous reagents that undergo self-terminating surface reactions. Various possible

approaches for copper ALD have been studied. A wide range of copper precursors have been tested with traditional reducing agents like hydrogen, formaldehyde and alcohols<sup>2a,2b</sup>. Orimoto *et al.*<sup>3</sup> conducted a screening study on various copper(II)  $\beta$ -diketonates using DFT to estimate complex stabilities. They found that although the calculations were done without full consideration of the environment, they still could correctly predict the stability values from the literature and from cyclic voltametry. Thus, we conclude that DFT is an efficient method to investigate the ALD reactions.

Cu(I) compounds are described by Li *et al.*<sup>4</sup> as promising precursors for Cu ALD, but later through the study of Ma *et al.*<sup>5</sup>, we see that these reactions resemble thermal chemical vapor deposition (CVD) rather than ALD as the molecules have the tendency to self decompose at the surface. Coyle *et al.*<sup>6</sup> have described a similar type of reaction in a DFT and FTIR study. Simple precursors like copper chloride with hydrogen as the reducing agent have been computed by Per *et al.*<sup>7</sup>, both in the gas phase and also over a copper (111) surface. They describe the formation of HCl along with deposition of copper over the surface. The low volatility of CuCl might be a problem for the reaction. But the problem of islanding remains, due to the high thermal energy needed to crack the hydrogen molecule. There are also reports of plasma enhanced ALD of copper by Wu *et al.*<sup>8</sup> where the use of hydrogen plasma prior to copper ALD enhances nucleation and promotes (111)-textured growth<sup>9</sup>.

A good replacement of the traditional reducing agents by an organometallic compound is reported by Lee *et al.*<sup>10</sup>, who achieved copper deposition by the alternate and separate pulsing of copper dimethyl-2-propoxide  $\text{Cu}(\text{dmap})_2$  and diethylzinc at 120°C. They have suggested that the precursor adsorbs on the surface through dipole-dipole interaction and have proposed the following transmetallation reaction:



The by-products have been reported by them to desorb from the surface without decomposition at the low temperature. The use of a liquid co-reagent makes it possible to perform solution phase

screening and so Vidjayacoumar *et al.*<sup>11</sup> have examined the possibility of these kinds of ligand exchange reactions for deposition of copper from solution with organometallic reagents like trimethylaluminium and triethylborane as well as diethylzinc. They have also checked a wide range of ligands: copper(II) acetylacetonate  $\text{Cu}(\text{acac})_2$ , copper(II)hexafluoroacetylacetonate  $\text{Cu}(\text{hfac})_2$ , copper(II)N-isopropyl-2-pyrrolyl-aldiminate  $\text{Cu}(\text{PyrIm}^{\text{iPr}})_2$  and copper(II)N-ethyl-2-pyrrolyl-aldiminate  $\text{Cu}(\text{PyrIm}^{\text{Et}})_2$ . Intermediates like  $\text{LMEt}$  ( $\text{M} = \text{Cu}, \text{Zn}$ ,  $\text{L} = \text{ligand}$ ),  $\text{Cu}_2\text{L}_2$  and  $\text{LEt}$  have been detected in solution when diethylzinc was the reducing agent. Corresponding intermediates using trimethylaluminium and triethylborane were also detected in the solution phase study. They have come to the conclusion that diethylzinc is the best of the reducing agents due to its high reactivity compared to the other organometallic reagents that they have studied.

Understanding the mechanism of Cu ALD by transmetallation is the motivation for this work. The intermediates found during the course of analogous reactions in solution<sup>11-12</sup> give a first picture for the reaction pathway. However, an improved understanding of the mechanism at its atomic level will help us to find a better precursor and identify the problems related to existing organometallic reagents as the reducing agent. For this we have taken into consideration the same precursors used by Vidjayacoumar *et al.* along with the copper(II)dialkylamino-2-propoxide  $\text{Cu}(\text{dmap})_2$  that has been studied by Lee *et al.* (Figure 1).  $\text{CuCl}_2$  data have also been calculated so as to find out about the simplest form of ligand. As co-reagent we consider diethylzinc. An assumption has been made here that all the ligands in the copper precursors are “innocent”, meaning that they themselves are neither oxidizing nor reducing<sup>13</sup>.

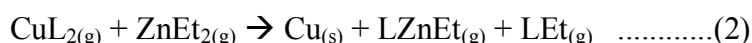
In chemistry the reaction pathway is the step by step sequence of the elementary reactions by which overall chemical change occurs. Only the net chemical change is directly observable for most chemical reactions and it is sometimes not possible to detect the individual steps. Atomic-scale calculations can be used to propose reactions pathways and assess their likelihood. In this paper, we use quantum chemical calculations of model molecules to analyze the various reaction pathways

across a range of copper precursors. Exothermic (downhill) reactions are represented as negative reaction energies and are assumed to be more probable than endothermic reactions. In fact, the probability of a reaction occurring depends on how frequently the reacting species can meet each other during the pathway and also the free energy of activation of the reaction steps, which includes changes in geometry needed for activation. We have chosen model molecules to represent metal-ligand bonding at various reaction steps, but we are aware that the geometries do not resemble those of surface-bound species during ALD growth. Hence, we do not attempt to compute activation energies. Instead, our arguments are based on the impossibility of highly endothermic steps and the expected abundance of reactants and intermediates.

The transmetallation mechanism can be divided into three types of reactions as illustrated with the following:

- Disproportionation:  $\text{Cu(I)}_2\text{L}_2 \rightarrow \text{Cu(II)L}_2 + \text{Cu(0)}$
- Ligand exchange:  $\text{CuL}_2 + \text{ZnEt}_2 \rightarrow \text{CuLEt} + \text{ZnLEt} \rightarrow \text{CuEt}_2 + \text{ZnL}_2$
- Reductive elimination:  $\text{Et}^- \rightarrow \text{Et}^+ + 2\text{e}^-$

One of the main aims in this paper is to understand how these reactions combine in the overall ALD reaction (Eq.1) to form elemental copper. We also seek to find out whether alternative overall reactions are possible, such as:



The formation of LEt and LZnEt as by-products is observed by Vidjayacoumar *et al.*<sup>11-12</sup> in solution phase, but these by-products have not been reported by Lee *et al.*<sup>14</sup> in the gas-surface ALD scenario. Through our study we see that Cu(I)L species (modelled by gas-phase  $\text{Cu}_2\text{L}_2$ ) are important intermediates and thus have been studied extensively. Another way for Cu to form is by disproportionation of the Cu(I) intermediate  $\text{Cu}_2\text{L}_2$  but disproportionation involves no net transfer of electrons and hence cannot be a growth reaction.

## Methods

Our focus in this study is on the differences in geometry and bonding strength of the various copper precursors. The precursor molecules  $\text{CuL}_2$ ,  $\text{ZnEt}_2$  and their ALD reaction products were modeled as isolated molecules in vacuum. We also used the gas-phase model to investigate molecules such as  $\text{CuLEt}$  and  $\text{Cu}_2\text{L}_2$  that crudely resemble the oxidation state and bonding in likely reaction intermediates occurring on the growing surface during ALD. A later study will develop a more realistic surface model.

The ground state electronic wave function of each molecule was calculated self-consistently within Kohn-Sham density functional theory (DFT) using the TURBOMOLE suite of quantum chemical programs<sup>15a,b</sup>. The Perdew-Burke-Ernzerhof (PBE) functional<sup>16</sup> with the resolution-of-the-identity approximation (RI)<sup>17,18</sup> and valence double-zeta with polarization def-SV(P) basis set<sup>19</sup> was considered the most suitable level of calculation, a good trade-off between accuracy and cost. For instance, in the case of  $\text{Cu}(\text{dmap})_2$ , the calculations performed at this level showed an expected level of agreement with experimental bond distances for Cu-O (1.91 Å theory, 1.86 Å exp) and Cu-N (2.09 Å theory, 2.06 Å exp)<sup>19</sup>. The coordination environment around copper is computed to be planar in this molecule, as observed by experiment. All the Cu(II) precursor molecules are open shell compounds and the Cu(I) compounds are closed shell. The Zn(II) compounds are closed shell compounds and the Zn(I) are open shell. The open shell compounds were computed using unrestricted DFT.

The entropy of selected precursors and the corresponding by-products has been calculated at 120°C using vibrational analysis in TURBOMOLE<sup>20</sup>. This calculation helps us to determine the influence of temperature on the free energy of adsorption or desorption.

The most serious error in this gas-phase approach probably comes from using the isolated Cu(0) atom as a model for metallic Cu. Therefore to correct this, we have calculated both bulk Cu and the atom using a periodic code with the same density functional theory and we correct the gas-

phase values by adding this energy difference  $\Delta E(\text{Cu}_{(\text{g})} \rightarrow \text{Cu}_{(\text{s})})$ . For this we have done a plane wave calculation using the VASP code<sup>21</sup> in which the valence electron states are expanded in a plane-wave basis set with an energy cutoff of 300 eV<sup>22</sup>. The electron exchange and correlation were treated within the same PBE functional. For the bulk copper, k-point sampling is performed with 8×8×8 Monkhorst-Pack sampling grid. The bulk lattice constant is determined using the Murnaghan equation of state. The additional energy has been added to the reaction steps which have metallic copper formation. The same energy correction has been added to the reaction steps where metallic zinc is formed, although our interest is not in zinc formation *per se*.

## Results

### **Structures of Cu and Zn compounds**

Selected parameters for the optimized structures of the Cu(II) precursors and the corresponding Zn(II) compounds are presented in Table 1. The computed bond lengths between metal and O are practically the same for the M(acac)<sub>2</sub> and M(hfac)<sub>2</sub> compounds (1.95-1.97 Å). As shown in Figure 2, the Cu complexes are planar (dihedral angle of 0-6° between four O atoms), consistent with the Cu(II):d<sup>9</sup> electronic structure, whereas the Zn analogues are distorted tetrahedral (dihedral angle ~75°), due to Zn(II):d<sup>10</sup>. The computed structures of M(dmap)<sub>2</sub> are similar, although the M-O distance is shorter (1.89-1.91 Å), consistent with more anionic O. The computed frequency for the vibration of the Cu(II) atom out of the plane is 43 cm<sup>-1</sup> for Cu(dmap)<sub>2</sub> and 34 cm<sup>-1</sup> for Cu(acac)<sub>2</sub> precursors.

Bonding in the pyrrolylaldiminates is quite different. For Cu(PyrIm<sup>R</sup>)<sub>2</sub> precursors, the bond length from Cu to the pyrrole nitrogen (1.98 Å) is smaller than that to the imine nitrogen (2.04-2.06 Å), but it is the reverse in the corresponding zinc compound (2.06 Å and 2.00-2.01 Å respectively). This indicates different resonance forms of the ligand when bound to Cu versus Zn, although there is probably substantial delocalization of negative charge in both cases within the plane of the ligand backbone. The Cu(PyrIm<sup>R</sup>)<sub>2</sub> complexes are distorted substantially out of planarity around the Cu



centre (dihedral angles  $45^\circ$  and  $33^\circ$  for  $R=iPr$  and  $R=Et$  respectively), which is likely to cause strain in the electronic structure. Finally the monodentate complexes are computed to be bent ( $CuEt_2$ ) or linear ( $CuCl_2$ ,  $ZnEt_2$ ,  $ZnCl_2$ ).

One of the proposed intermediates for the reaction is  $Cu_2L_2$ <sup>12</sup>. We find that these are Cu(I) compounds, most stable when computed as closed shell singlets. As reported in other works on copper precursors,<sup>6, 12</sup>  $Cu_2L_2$  are an interesting set of compounds, occurring in a variety of structures in terms of dihedral angle and intra-molecular Cu-Cu distance. The common feature is linear coordination about the  $Cu(I):d^{10}$  centre. Our structural results for dimeric Cu(I) complexes using the same ligands and their Zn(I) analogues are shown in Table 2 and depicted in Figure 3. The intra-molecular Cu-Cu distance is short (2.4-2.5 Å,  $L=dmap$ ,  $PyrIm$ ), suggesting a bonding interaction, or longer in the case of a Cu-O-Cu bridge (3.0-3.1 Å,  $L=acac$ ,  $hfac$ ). In the cases of  $L=acac$  and  $L=hfac$ , one side of each bidentate ligand forms the Cu-O-Cu bridge and the complex is planar. By contrast, each ligating atom in  $L=dmap$  and  $L=PyrIm$  is coordinated to just one metal centre and the resulting structures are distorted out of planarity (e.g.  $24^\circ$  Cu-N-N-Cu dihedral angle for  $L=PyrIm^{iPr}$ ), probably due to steric interaction in the ligand sphere (Figure 2). The out of plane vibration of Cu atom in  $Cu_2(dmap)_2$  is computed to have a frequency of  $44\text{ cm}^{-1}$ . It is interesting to note the near-identical Cu-N distances in the pyrrolylaldiminates (1.88-1.90 Å) that indicate equal charge on the N atoms in the Cu(I) dimer. Overall we see that similar kinds of precursors have similar structures:  $Cu_2(acac)_2$  and  $Cu_2(hfac)_2$  can be grouped together and  $Cu(PyrIm^R)_2$   $R=iPr$  and  $R=Et$  can form another group.

The computed entropy of the precursor and the by-products is reported in Table 3. The data show approximately equal entropy for zinc and copper molecules, indicating similar trends in adsorption or desorption with temperature. This is undesirable from the ALD viewpoint, as the zinc compounds might co-deposit along with the copper compounds. The butane molecule has less entropy than  $LEt$  and so is less sensitive to thermal effects during desorption. Breaking down the entropy calculation,

we see that there is a contribution of ~33% from translational motion, ~27% from rotational motion and ~40% from vibrational motion in most of the cases.

## **Reaction Mechanism**

The computed energetics of the proposed reaction steps are listed in Table 4. Our starting point is the interconversion of Cu(0), Cu(I) and Cu(II) when complexed to the various ligands. Considering step I, we see that disproportionation of  $\text{Cu(I)}_2\text{L}_2$  into  $\text{Cu(0)}_{(\text{s})}$  and  $\text{Cu(II)L}_2$  is thermodynamically favored when  $\text{L}=\text{acac}$ ,  $\text{hfac}$ ,  $\text{dmap}$  and  $\text{Et}$ . For both  $\text{L}=\text{PyrIm}$  complexes on the other hand, the data show a driving force for  $\text{Cu(II)L}_2$  to be reduced to  $\text{Cu(I)}_2\text{L}_2$  in the presence of  $\text{Cu(0)}$ , as might occur on adsorption onto a Cu surface during ALD.

We assume that none of the ligands are reducing agents except  $\text{Et}^-$  and the simulations support this assumption. Reduction of copper is therefore only possible after exchanging a non-reducible ligand L for Et from Zn. Steps II and III in Table 4 are stepwise ligand exchange reactions for Cu(II) and Zn(II). The reactions are energetically neutral (within  $\pm 10$  kJ/mol) for  $\text{L}=\text{acac}$  and  $\text{PyrIm}^{\text{iPr}}$  and show moderate exothermicity and endothermicity ( $< 20$  kJ/mol) in both steps for  $\text{L}=\text{hfac}$  and  $\text{PyrIm}^{\text{Et}}$  respectively, implying that the changes in bonding in Cu(II) and Zn(II) are quite evenly matched.  $\text{Cu(dmap)}_2$  is seen to resist exchange of its first ligand by 50 kJ/mol, but not its second. The opposite is the case for  $\text{L}=\text{Cl}$ , where exchange of the first ligand is favored, but not the second. By contrast, exchanging L and Et between Cu(I) and Zn(II) (both  $d^{10}$ ) is found to cost energy for all ligands, ranging from +9 kJ/mol for  $\text{L}=\text{acac}$  to +97 kJ/mol for  $\text{L}=\text{PyrIm}^{\text{iPr}}$  (steps IV and V, Table 4).

Steps VII-X are possible redox reactions by which the  $\text{Et}^-$  ligand is oxidized to cationic  $\text{Et}^+$ , combines with an anion and is eliminated, while the Cu(II) or Cu(I) centre is reduced to Cu(I) or Cu(0). The computed energetics for  $\text{CuEt}_2$  form a baseline: reduction from Cu(II) to Cu(I) yields -226.4 kJ/mol per Cu (step VII or IX) and further reduction from Cu(I) to solid Cu(0) yields -388 kJ/mol (step X), with butane ("Et-Et") as the by-product.

Considering the other ligands in a mixed complex of the type  $\text{Cu(II)LEt}$ , step VII is the redox reaction  $\text{Cu(II)} \rightarrow \text{Cu(I)} + \text{butane}$ . The computed energies are very negative for all L (-134 to -186 kJ/mol of Cu), meaning that the reaction is highly thermodynamically favored, even more so than  $\text{CuEt}_2$ . This can be traced back to the tendency for disproportionation of the various  $\text{Cu}_2\text{L}_2$  complexes. The most exothermic reactions are for the pyrrolylaldiminates. Alternatively, LEt can be produced from such mixed complexes by the complete reduction  $\text{Cu(II)} \rightarrow \text{Cu(0)}_{(\text{s})}$  (step VIII) and this is somewhat less thermodynamically favorable (-73 to -165 kJ/mol-Cu). It is to be noted that in PyrIm cases, it is favored for the  $\text{Et}^+$  to be attached to the  $\text{N}_{\text{pyr}}$  and not  $\text{N}_{\text{im}}$ . Butane (step VII) is therefore the thermodynamically favored by-product of reductive elimination from two neighboring  $\text{Cu(II)LEt}$ . Step VIII can be broken down into step IX producing Cu(I) followed by step X. So, by construction, step VIII is half the reaction energy of the sum of step IX and step X. Loss of LEt from Cu(II) complexes (step IX) is favored only for  $\text{L}=\text{dmap}$ , PyrIm, and with a lower  $\Delta E$  than loss of butane (step VII). Loss of LEt from Cu(I) complexes (step X) is favored for all L. Of course, there is an unknown kinetic barrier associated with the structural and electronic changes needed to bring  $\text{Et}^+$  to bond with O or N of the ligand L so as to form LEt.

Even though they may not be desirable in ALD, the same reactions are in principle possible for Zn as for Cu, and the computed data for Zn complexes are shown in Table 5. To the best of our knowledge, Zn(I) complexes have not yet been isolated and they are therefore only regarded as potential intermediates in this reaction mechanism.

Disproportionation (step I) of  $\text{Zn}_2\text{L}_2$  is thermodynamically favored for both PyrIm ligands ( $\Delta E=-83$  and  $-100$  kJ/mol of  $\text{Zn}_2\text{L}_2$ ), is energetically neutral for  $\text{L}=\text{dmap}$  and is not favored for  $\text{L}=\text{acac}$ ,  $\text{hfac}$ , Cl and Et. The ligands thus behave in roughly the opposite way compared with disproportionation of Cu. In particular,  $\Delta E=+33$  kJ/mol for  $\text{Zn}_2\text{Et}_2$  means that the reverse reaction – ligand transfer from  $\text{ZnEt}_2$  to  $\text{Zn(0)}$  – will be favored.

Clearly, the energetics for ligand exchange from Zn(II) to Cu(II) (steps II and III, Table 4) must by definition mirror those for Cu(II) to Zn(II) (Table 5). However there are some differences for Zn(I)/Cu(II) ligand exchange (steps IV and V), which can be exothermic in both steps (L=PyrIm), near neutral (L=dmap) or endothermic in the first step and exothermic in the second (L=acac, hfac). We find both Zn(I) and Cu(II) to have unpaired electrons on the metal centre.

Reductive elimination of ligands from Zn complexes is also substantially different to that from Cu. The baseline values for decomposition of  $\text{ZnEt}_2$  to  $\text{Zn(0)}_{(\text{s})}$  (+155 kJ/mol per Zn, step VIII) and  $\text{Zn}_2\text{Et}_2$  to  $\text{Zn(0)}_{(\text{s})}$  (+102 kJ/mol-Zn, step X) show that reduction to Zn metal and butane is not favorable, unlike Cu. In line with this, the calculations show that reductive elimination from most Zn-L complexes is endothermic. The reduction reaction forming butane is moderately favored in some cases (step VII: -95, -97 and -33 kJ/mol for L=acac, hfac, dmap respectively) but not for L=PyrIm, in contradiction of the trend for Cu-L. As in the case of Cu, the formation of butane is favored over formation of L<sub>2</sub>Et as the by-product of reduction of Zn.

## Discussion

### **Geometry of the compounds:**

Cu(II) complexes favor a planar geometry because of the Cu(II):d<sup>9</sup> electronic configuration, but in molecules like  $\text{Cu}(\text{PyrIm}^{\text{R}})_2$ , high steric hindrance between the two rigid ligands means that the molecules distort out of planarity. These effects are explained by Raithby *et al.*<sup>23</sup>. In the  $\text{Cu}_2\text{L}_2$  compounds the Cu-O/N bonds are shorter (and hence probably stronger) than those of the  $\text{CuL}_2$  counterparts, despite lower cationic charge on Cu. This seems to reflect less steric hindrance between ligands that are arranged around a larger core of two Cu atoms. In addition, each Cu(I):d<sup>10</sup> adopts linear coordination that is more flexible than the planar Cu(II) case. In this way, we see that L=PyrIm favors Cu(I) over Cu(II), explaining the driving force towards partial reduction in the presence of bulk Cu(0) (reaction steps VII and IX) and against disproportionation (step I, Table 4). L=acac, hfac also have a rigid backbone, but in contrast with L=PyrIm, the CH<sub>3</sub>

and  $\text{CF}_3$  groups are arranged away from the Cu(II) centre and cause less steric hindrance.  $\text{L}=\text{dmap}$  is also relatively flexible within the Cu(II) coordination sphere. This means that there is little distortion out of planarity, and hence less driving force towards reduction of Cu(II) for  $\text{L}=\text{acac}$ ,  $\text{hfac}$  and  $\text{dmap}$ . It is therefore favorable for  $\text{Cu}_2\text{L}_2$  to disproportionate into  $\text{CuL}_2$  and Cu(0) in these cases and this may be a route by which Cu(0) is formed. We speculate that the planar precursors with rigid ligands  $\text{Cu}(\text{acac})_2$  and  $\text{Cu}(\text{hfac})_2$  may resist the distortion that would be necessary for the Cu centre to approach a planar substrate and adsorb. An alternative adsorption mode for all  $\text{CuL}_2$  would be via the ligand, which because it is bidentate could bridge surface-Cu and adsorbate-Cu. Explicit calculations of molecule surface adsorption will be needed to clarify these points.

The Cu(I) intermediates  $\text{Cu}_2\text{L}_2$  have various bonding characteristics. In case of PyrIm and  $\text{dmap}$  precursors, the ligand binds to two copper atoms. The bonding in case of  $\text{acac}$  type precursors is different: the ligand not only binds to the two copper atoms but one of the ligand O atoms bridges two copper atoms at the same time. The metal-ligand bond lengths are different in each of the cases, as stated in Table 2. The molecule that appears to be least rigid is  $\text{Cu}_2(\text{dmap})_2$ . This may mean that the  $\text{dmap}$  precursor can be adsorbed onto a surface via a Cu(I) intermediate more easily than the others. This is due to the absence of conjugation in the ligand as well as less steric hindrance between ligands.

## **Reactions**

The most thermodynamically favorable gas phase reactions in both the pulses are depicted in Figure 3. It shows a general overview of the reactions that might take place irrespective of the precursors used.

Precursor Pulse - In an ALD reaction, during the first pulse of the precursor over the surface, the copper might disproportionate from Cu(II) in the precursor and from Cu(0) of the surface to form a Cu(I) dimer, as seen in the reverse case of step I in Table 3. The possibility for this reaction to occur is high for the PyrIm precursors as shown by its exothermicity and low for  $\text{acac}$ ,  $\text{hfac}$  and  $\text{dmap}$

precursors (small endothermicity). Therefore, after the precursor pulse, a saturated Cu(I) surface is expected, especially for PyrIm. These data reveal nothing about kinetics; there might be differences in the rates of reaction and in the time needed to saturate Cu(I) over the surface. The reverse reaction, disproportionation, might take place during the purge step as the excess  $\text{CuL}_2$  is purged out of the system. Here acac, hfac and dmap are the most likely precursors to undergo this reaction and revert to Cu(0).

Reducing agent pulse - During the reducing agent pulse, diethylzinc approaches a surface saturated with Cu(I). It can follow the slightly endothermic reaction (step IV) to yield  $\text{Cu}_2\text{LEt}$  and  $\text{LZnEt}$ . The following reaction (step V) can only take place if the product  $\text{ZnL}_2$  is very volatile and can be easily purged out of the system. Judging by the thermodynamics of the reactions, we can say that step V is probably less favorable for PyrIm precursors than for the rest of the precursors. However, we see from Table 3 that the ligand exchange for Cu(II) (steps II and III) is more favorable than for Cu(I) (steps IV and V) in most of the cases of the different precursors that have been studied here. Thus, if unreacted Cu(II) precursor is left in the system, it will undergo half ligand exchange to produce  $\text{LCuEt}$  and  $\text{LZnEt}$ . Further, a competition between reductive elimination and ligand exchange will arise (step III and step VII). If reductive elimination is kinetically faster than ligand exchange, it will produce a Cu(I) saturated surface, which we denote  $\text{Cu}_2\text{L}_2$ . On the other hand, if reductive elimination is slower than ligand exchange, there is the possibility of complete exchange to give  $\text{CuEt}_2$  and  $\text{ZnL}_2$  (step III). The probability of ligand exchange can be increased by increasing the concentration of diethylzinc in this case. If the produced  $\text{ZnL}_2$  is volatile, it will drive step III forwards following Le Chatelier's principle. The  $\text{CuEt}_2$  product is stable against reduction and hence step III reduces the probability of formation of copper metal. Hence, we can say that a complete ligand exchange between Cu(II) and Zn(II) without the intermediate formation of Cu(I) is to be avoided due to the formation of stable  $\text{CuEt}_2$  at the end of the reaction.

The simultaneous formation of  $\text{Cu}_2\text{Et}_2$  along with  $\text{ZnL}_2$  in step V helps in the formation of metallic copper, since  $\text{Cu}_2\text{Et}_2$  can then undergo reductive elimination (as seen in step X when  $\text{L}=\text{Et}$ ) to yield butane and metallic copper. In case the products of step IV,  $\text{Cu}_2\text{LEt}$  and  $\text{LZnEt}$ , are allowed to accumulate at the surface,  $\text{Cu}_2\text{LEt}$  will probably dissociate to give metallic copper and  $\text{LEt}$ , as all these reactions for the different ligands are exothermic in nature. However,  $\text{LZnEt}$  might form the dimer  $\text{Zn}_2\text{L}_2$  and butane gas as seen in step VII. The dimer  $\text{Zn}_2\text{L}_2$  might accumulate in the system for acac and hfac type precursors but it will disproportionate into  $\text{Zn}$  and  $\text{ZnL}_2$  for the rest of the precursors. Thus there is more probability of  $\text{Zn}$  contamination in the case of PyrIm type precursors.

In all the reactions quoted in Table 4 and 5, we find that the most thermodynamically-preferred by-product is butane rather than  $\text{LEt}$  for similar types of reaction (step VII and step VIII). However, the probability of formation of  $\text{LEt}$  cannot be ignored as the computed reaction energy is exothermic. Of course, kinetics and surface concentrations will dictate which product actually occurs; *i.e.* whether  $\text{LEt}$  eliminates from a single  $\text{LCuEt}$  unit (step VIII) or whether butane can form from adjacent  $2\text{LCuEt}$  (step VII). Entropy data show us that once the  $\text{LEt}$  is formed then it has more probability of being desorbed from the surface at elevated temperatures, as it has higher entropy. Thus, if  $\text{LCuEt}$  is not allowed to accumulate in the system,  $\text{LEt}$  formation is favorable. The  $\text{LEt}$  has some probability of decomposing into  $\text{LH}$  and  $\text{C}_2\text{H}_4$  (step IX) but in all the cases for different precursors we see that this reaction is less favored, with the reaction energy increasing from acac type precursors to the PyrIm type.

We conclude that the surface after the reducing agent pulse in ALD is saturated with either  $\text{Cu}_2\text{Et}_2$  or  $\text{Zn}_2\text{L}_2$  type species.  $\text{Cu}_2\text{Et}_2$  is unstable and gives metallic copper and diethylcopper. Reduction of  $\text{Cu(II)}$  to  $\text{Cu(0)}$  is generally energetically favored over reduction of  $\text{Zn(II)}$  to  $\text{Zn(0)}$  as observed in step I and VIII in Table 4 and Table 5.

As the concentration of ligands and metals changes on the surface during an ALD experiment, we expect different reaction steps to predominate. For instance, we expect complete copper ligand

exchange to be favored when diethylzinc is in excess during the reducing agent pulse as seen in steps III and V. The likely by-products are butane (after the decomposition of  $\text{Cu}_2\text{Et}_2$  as seen in step X),  $\text{ZnL}_2$  and some  $\text{CuEt}_2$ . On the other hand, the high concentration of  $\text{CuL}_2$  in the Cu precursor pulse will cause reductive elimination of Et fragments resulting in Cu(I) species like  $\text{Cu}_2\text{L}_2$  or  $\text{Cu}_2\text{LEt}$  as in steps VII and IX. The probable by-products are LEt and butane. Thus we see the pathway that was proposed by Lee *et al.* for the formation of copper in its metallic form, equation (1), is only favored when there is an excess of the reducing agent  $\text{ZnEt}_2$ .

Choice of ligands: During exposure to PyrIm precursors, the formation of a Cu(I) intermediate on the surface is favorable, but in the subsequent reducing steps, the co-deposition of zinc metal along with copper is likely to take place. Thus, although PyrIm precursors enjoy the benefit of not having any oxygen in the ligand, which reduces the probability of formation of copper oxide in any of the steps, the probability of zinc formation is high. We suggest that this can be avoided if the  $\text{LZnEt}$  intermediate is not allowed to accumulate in the system. For instance, a volatile  $\text{ZnL}_2$  by-product might carry reaction step V in the forward direction and thus prevent the accumulation of  $\text{LZnEt}$ .

For acac and hfac precursors, the initial step of formation of  $\text{Cu}_2\text{L}_2$  might be slow as the computed model reaction is endothermic. During the reducing agent pulse, the formation of copper in its metallic form is probably favorable as the important reaction steps in our model are exothermic in nature. However, a saturated surface of  $\text{Zn}_2\text{L}_2$  is expected along with copper metal.

The dmap precursor follows the same trend as the acac and the hfac precursors. Here a simultaneous co-deposition of copper and zinc is likely, although the copper deposition is favored in terms of reaction energy.

Based on this study of the transmetallation reaction with diethylzinc, we suggest that one of the best methods of improving the transmetallation reaction at low temperatures is to choose a ligand that makes the  $\text{ZnL}_2$  species very volatile. If this molecule can be continuously purged out of the system it will drive the reaction forward and simultaneously produce Cu(0). Accumulation of  $\text{LZnEt}$



might prove harmful as it might dimerize to give  $\text{Zn}_2\text{L}_2$ , which dissociates to give zinc metal in cases like PyrIm and also forms a saturated surface of  $\text{Zn}_2\text{L}_2$  in other cases.

Transmetallation can also be improved by choosing a metal in the reducing agent which is less likely to be co-deposited along with copper, i.e. the metals far away from copper in the electrochemical series. Reducing agents containing transition metals like vanadium, chromium or manganese might be helpful.

A complete ligand exchange with diethylzinc is to be avoided as it will lead to the formation of  $\text{Cu(II)Et}_2$ , which is stable and hence does not give metallic copper. Therefore the formation of copper via a  $\text{Cu(I)}$  intermediate should be targeted and this can be achieved by reductive elimination of  $\text{Cu(II)}$  intermediates to give either butane or  $\text{LEt}$  gaseous by-products.

None of the precursors studied here is ideal as they all have advantages and disadvantages. We find that the dmap precursor is preferred over the others due to the flexibility of the ligand, less probability of co-deposition of the zinc metal and exothermic reaction energies in the important reaction steps.

## Conclusion

We have used DFT to study the geometry and energetics of precursors and model intermediates during the reaction steps involved in the transmetallation ALD of Cu using diethylzinc. The reaction steps are disproportionation, ligand exchange and reductive elimination. We have investigated the effect of various ligands or the ethyl group on the stability of intermediates and by-products, including those of  $\text{Cu(II)}$ ,  $\text{Cu(I)}$  and  $\text{Cu(0)}$  via model molecules.

Through our study we have seen that the choice of precursor ligand (L) strongly affects the structure of the  $\text{Cu(I)}_2\text{L}_2$  intermediate, which plays a decisive role in determining the mechanism of copper deposition. However similar kinds of ligands can be grouped together and have similar features.

After the Cu(II) precursor pulse we predict that the surface is probably covered with a Cu(I)L-like intermediate. During the reducing agent pulse, a complete ligand exchange between Cu(II) and Zn(II) is to be avoided as it will result in a stable CuEt<sub>2</sub> compound, i.e. without the formation of a Cu(I) intermediate. The formation of butane gas (Et-Et) is more likely than LEt as a by-product. When ZnL<sub>2</sub> is volatile it will carry the reaction forward. Contamination of the film can occur in the form of adsorbed Zn(L)-like intermediates or Zn in its metallic state.

Thus, although the proposal to use an organometallic reagent as the reducing agent for copper ALD was an innovative idea by Lee *et al.*, the specific use of diethylzinc may result in zinc contamination as zinc is close to copper in the electrochemical series. Other reducing reagents which have metals far away from copper in the series should be considered as alternatives.

The above reaction pathway shows the difference between the commonly used precursors. The electronegativity, steric hindrance and the aromaticity present in the ligands all play important roles in deciding the direction of flow of the reactions. Of the set studied here, Cu(dmap)<sub>2</sub> is probably the best and Cu(PyrIm<sup>R</sup>)<sub>2</sub> the worst to be used as a precursor in this process.

ACKNOWLEDGMENT: Thanks to Science Foundation Ireland for funding under the ALDesign project, grant number 09.IN1.I2628, <http://www.tyndall.ie/aldesign>, and to R. Nagle, S. Clendenning and H. Simka of Intel Corporation for useful discussions. Y. Maimaiti is thanked for carrying out calculations of bulk Cu.

#### References:

1. *International Technology Roadmap for Semiconductors*. 2011.
2. (a) Cabañas, A.; Shan, X.; Watkins, J. J., Alcohol-Assisted Deposition of Copper Films from Supercritical Carbon Dioxide. *Chemistry of Materials* **2003**, *15* (15), 2910-2916; (b) Soininen, P. J.; Elers, K. E.; Saanila, V.; Kaipio, S.; Sajavaara, T.; Haukka, S., Reduction of Copper Oxide Film to Elemental Copper. *Journal of the Electrochemical Society* **2005**, *152* (2), G122-G125.
3. Orimoto, Y.; Toyota, A.; Furuya, T.; Nakamura, H.; Uehara, M.; Yamashita, K.; Maeda, H., Computational Method for Efficient Screening of Metal Precursors for Nanomaterial Syntheses. *Industrial & Engineering Chemistry Research* **2009**, *48* (7), 3389-3397.

4. Li, Z.; Barry, S. T.; Gordon, R. G., Synthesis and Characterization of Copper(I) Amidinates as Precursors for Atomic Layer Deposition (ALD) of Copper Metal. *Inorganic Chemistry* **2005**, *44* (6), 1728-1735.
5. Ma, Q.; Guo, H.; Gordon, R. G.; Zaera, F., Surface Chemistry of Copper(I) Acetamidinates in Connection with Atomic Layer Deposition (ALD) Processes. *Chemistry of Materials* **2011**, *23* (14), 3325-3334.
6. Coyle, J. P.; Johnson, P. A.; DiLabio, G. A.; Barry, S. n. T.; Muller, J., Gas-Phase Thermolysis of a Guanidinate Precursor of Copper Studied by Matrix Isolation, Time-of-Flight Mass Spectrometry, and Computational Chemistry. *Inorganic Chemistry* **2010**, *49* (6), 2844-2850.
7. (a) Mårtensson, P.; Larsson, K.; Carlsson, J.-O., Atomic layer epitaxy of copper: an ab initio investigation of the CuCl/H<sub>2</sub> process: III. Reaction barriers. *Applied Surface Science* **2000**, *157* (1-2), 92-100; (b) Mårtensson, P.; Larsson, K.; Carlsson, J.-O., Atomic layer epitaxy of copper: an ab initio investigation of the CuCl/H<sub>2</sub> process: I. Adsorption of CuCl on Cu(111). *Applied Surface Science* **1998**, *136* (1-2), 137-146; (c) Mårtensson, P.; Larsson, K.; Carlsson, J.-O., Atomic layer epitaxy of copper: an ab initio investigation of the CuCl/H<sub>2</sub> process: II. Reaction energies. *Applied Surface Science* **1999**, *148* (1-2), 9-16.
8. Wu, L.; Eisenbraun, E., Effects of hydrogen plasma treatments on the atomic layer deposition of copper. *Electrochemical and Solid State Letters* **2008**, *11* (5), H107-H110.
9. Wu, L.; Eisenbraun, E., Hydrogen plasma-enhanced atomic layer deposition of copper thin films. *Journal of Vacuum Science & Technology B* **2007**, *25* (6), 2581-2585.
10. Lee, B. H.; Hwang, J. K.; Nam, J. W.; Lee, S. U.; Kim, J. T.; Koo, S.-M.; Baunemann, A.; Fischer, R. A.; Sung, M. M., Low-Temperature Atomic Layer Deposition of Copper Metal Thin Films: Self-Limiting Surface Reaction of Copper Dimethylamino-2-propoxide with Diethylzinc. *Angewandte Chemie International Edition* **2009**, *48* (25), 4536-4539.
11. Vidjayacoumar, B.; Emslie, D. J. H.; Clendenning, S. B.; Blackwell, J. M.; Britten, J. F.; Rheingold, A., Investigation of AlMe<sub>3</sub>, BEt<sub>3</sub>, and ZnEt<sub>2</sub> as Co-Reagents for Low-Temperature Copper Metal ALD/Pulsed-CVD. *Chemistry of Materials* **2010**, *22* (17), 4844-4853.
12. Vidjayacoumar, B.; Emslie, D. J. H.; Blackwell, J. M.; Clendenning, S. B.; Britten, J. F., Solution Reactions of a Bis(pyrrolylaldimine)copper(II) Complex with Peralkyl Zinc, Aluminum, and Boron Reagents: Investigation of the Pathways Responsible for Copper Metal Deposition. *Chemistry of Materials* **2010**, *22* (17), 4854-4866.
13. Kaim, W., The Shrinking World of Innocent Ligands: Conventional and Non-Conventional Redox-Active Ligands. *European Journal of Inorganic Chemistry* **2012**, *2012* (3), 343-348.
14. Kim, H.; Lee, H. B. R.; Maeng, W. J., Applications of atomic layer deposition to nanofabrication and emerging nanodevices. *Thin Solid Films* **2009**, *517* (8), 2563-2580.
15. (a) Ahlrichs, R.; Bär, M.; Häser, M.; Horn, H.; Kölmel, C., Electronic structure calculations on workstation computers: The program system turbomole. *Chemical Physics Letters* **1989**, *162* (3), 165-169; (b) Schafer, A.; Huber, C.; Ahlrichs, R., Fully optimized contracted Gaussian basis sets of triple zeta valence quality for atoms Li to Kr. *The Journal of Chemical Physics* **1994**, *100* (8), 5829-5835.
16. Perdew, J. P.; Burke, K.; Ernzerhof, M., Generalized Gradient Approximation Made Simple. *Physical Review Letters* **1996**, *77* (18), 3865.
17. Eichkorn, K.; Weigend, F.; Treutler, O.; Ahlrichs, R., Auxiliary basis sets for main row atoms and transition metals and their use to approximate Coulomb potentials. *Theoretical Chemistry Accounts: Theory, Computation, and Modeling (Theoretica Chimica Acta)* **1997**, *97* (1), 119-124.
18. Sierka, M.; Hogekamp, A.; Ahlrichs, R., Fast evaluation of the Coulomb potential for electron densities using multipole accelerated resolution of identity approximation. *The Journal of Chemical Physics* **2003**, *118* (20), 9136-9148.
19. Becker, R.; Devi, A.; Weiß, J.; Weckenmann, U.; Winter, M.; Kiener, C.; Becker, H. W.; Fischer, R. A., A Study on the Metal Organic CVD of Pure Copper Films from Low Cost Copper(II)

Dialkylamino-2-propoxides: Tuning the Thermal Properties of the Precursor by Small Variations of the Ligand. *Chemical Vapor Deposition* **2003**, 9 (3), 149-156.

20. Deglmann, P.; May, K.; Furche, F.; Ahlrichs, R., Nuclear second analytical derivative calculations using auxiliary basis set expansions. *Chemical Physics Letters* **2004**, 384 (1-3), 103-107.

21. Kresse, G.; Hafner, J., Ab initio molecular-dynamics simulation of the liquid-metal–amorphous-semiconductor transition in germanium. *Physical Review B* **1994**, 49 (20), 14251-14269.

22. Kresse, G.; Furthmüller, J., Efficiency of ab-initio total energy calculations for metals and semiconductors using a plane-wave basis set. *Computational Materials Science* **1996**, 6 (1), 15-50.

23. Paul R. Raithby, G. P.; Shields, F. H. A. a.; Motherwell, W. D. S., Structure correlation study of four-coordinate copper(I) and (II) complexes. *Acta Crystallographica Section B* **1999**, 56.

Table 1- Optimized structural parameters of the copper precursors  $\text{CuL}_2$  and their corresponding zinc compounds  $\text{ZnL}_2$ . The dihedral angle is between the four coordinating atoms of the ligand, for example in  $\text{Cu}(\text{acac})_2$  the angle is between the four oxygen atoms  $\angle \text{O-O-O-O}$ .

	Bond Length (Å)	Dihedral Angle (°)	Bond Length (Å)	Dihedral Angle (°)
	$\text{CuL}_2$	$\text{CuL}_2$	$\text{ZnL}_2$	$\text{ZnL}_2$
$\text{M}(\text{acac})_2$	Cu-O:1.95	0.1	Zn-O:1.96	76.0
$\text{M}(\text{hfac})_2$	Cu-O:1.95	6.0	Zn-O:1.97	74.7
$\text{M}(\text{dmap})_2$	Cu-O:1.91 Cu-N:2.09	0.6	Zn-O:1.89 Zn-N:2.19	51.0
$\text{M}(\text{PyrIm}^{\text{R}})_2$ R=iPr	Cu-N <sub>pyr</sub> : 1.98 Cu-N <sub>im</sub> : 2.04	45.0	Zn-N <sub>pyr</sub> : 2.06 Zn-N <sub>im</sub> : 2.01	78.9
$\text{M}(\text{PyrIm}^{\text{R}})_2$ R=Et	Cu-N <sub>pyr</sub> :1.98 Cu-N <sub>im</sub> :2.06	33.0	Zn-N <sub>pyr</sub> :2.06 Zn-N <sub>im</sub> : 2.00	88.0

Table 2: Computed structural parameters for intermediate species  $\text{Cu}_2\text{X}_2$  and  $\text{Zn}_2\text{X}_2$ . The dihedral angle is between the two coordinating atoms of one ligand and the copper atoms, for example in  $\text{Cu}_2(\text{acac})_2$  the angle is between two oxygen atoms of one acac and the copper atoms  $\angle \text{Cu-O-O-Cu}$ .

	Cu-N/Cu-O (Å)	Cu-Cu (Å)	Dihedral Angle (°)	Zn-N/Zn-O (Å)	Zn-Zn (Å)	Dihedral Angle (°)
$\text{M}_2(\text{acac})_2$	Cu-O : 1.88	3.04	0.6	Zn-O : 1.98	2.33	0.6
$\text{M}_2(\text{hfac})_2$	Cu-O : 1.89	3.11	0.4	Zn-O : 2.00	2.33	0.35
$\text{M}_2(\text{dmap})_2$	Cu-O : 1.83/1.86 Cu-N:1.96/1.99	2.48	18.1	Zn-N : 1.90 Zn-O : 2.21/3.10	2.35	9.59
$\text{M}_2(\text{PyrIm}^{\text{R}})_2$ R= <sup>i</sup> Pr	Cu-N <sub>pyr</sub> : 1.88 Cu-N <sub>im</sub> :1.90	2.44	24.2	Zn-N <sub>pyr</sub> : 2.00 Zn-N <sub>im</sub> : 2.10	2.28	6.68
$\text{M}_2(\text{PyrIm}^{\text{R}})_2$ R=Et	Cu-N <sub>pyr</sub> : 1.88 Cu-N <sub>im</sub> :1.90	2.45	22.9	Zn-N <sub>pyr</sub> : 2.03 Zn-N <sub>im</sub> : 2.07	2.28	7.78

Table 3: Computed entropy (kJ/mol) of the precursors and the corresponding by-products calculated at 120°C.

Ligand (L)	CuL <sub>2</sub>	ZnL <sub>2</sub>	LEt
Acac	0.61	0.69	0.50
Dmap	0.69	0.70	0.48
PyrIm <sup>R</sup> R= <sup>i</sup> Pr	0.78	0.79	0.55
PyrIm <sup>R</sup> R=Et	0.71	0.72	0.50
Et	0.44	0.40	0.34

Table 4: Mechanism for the copper ALD is divided into three parts: ligand exchange, reductive elimination and disproportionation. The various reaction energies for different precursors are presented here.

Reaction		Step	$\Delta E$ (kJ/mol)						
			L=acac	L=hfac	L=dmap	L=PyrIm <sup>R</sup> R= <sup>i</sup> Pr	L=PyrIm <sup>R</sup> R=Et	L=Cl	L=Et
Disproportionation	$\text{Cu}_2\text{L}_2 \rightarrow \text{Cu} + \text{CuL}_2$	I	-31.4	-12.6	-34.6	71.3	61.1	21.4	-75.0
Ligand exchange for Cu(II)-Zn(II)	$\text{CuL}_2 + \text{ZnEt}_2 \rightarrow \text{LZnEt} + \text{LCuEt}$	II	4.7	-6.0	49.5	0.3	18.9	-34.9	
	$\text{LZnEt} + \text{LCuEt} \rightarrow \text{CuEt}_2 + \text{ZnL}_2$	III	-3.9	-14.9	2.6	-2.9	19.1	21.2	
Ligand exchange for Cu(I)-Zn(II)	$\text{Cu}_2\text{L}_2 + \text{ZnEt}_2 \rightarrow \text{LZnEt} + \text{Cu}_2\text{LEt}$	IV	43.0	44.0	47.6	51.9	51.1	33.2	
	$\text{Cu}_2\text{LEt} + \text{LZnEt} \rightarrow \text{Cu}_2\text{Et}_2 + \text{ZnL}_2$	V	9.2	27.3	39.7	96.9	84.1	49.4	
Ligand Exchange for Cu(II)-Cu(II)	$2\text{CuLEt} \rightarrow \text{CuL}_2 + \text{CuEt}_2$	VI	1.6	16.8	-48.2	5.0	-11.3	20.3	
Reductive elimination	$2\text{LCuEt} \rightarrow \text{Cu}_2\text{L}_2 + \text{Et-Et}$	VII	-268.3	-272.0	-315.0	-367.1	-373.1	-302.4	-226.4
	$\text{LCuEt} \rightarrow \text{Cu} + \text{LEt}$	VIII	-73.5	-74.3	-164.9	-109.1	-160.7	-164.3	-331.1
	$2\text{LCuEt} \rightarrow \text{Cu}_2\text{LEt} + \text{LEt}$	IX	26.2	18.3	-102.3	-98.2	-159.0	-87.7	-226.4
	$\text{Cu}_2\text{LEt} \rightarrow 2\text{Cu} + \text{LEt}$	X	-143.2	-136.8	-197.5	-90.0	-132.4	-211.2	-388.3
Decomposition reaction	$\text{LEt} \rightarrow \text{LH} + \text{C}_2\text{H}_4$	XI	38.5	59.7	149.3	152.6	113.9	125.7	147.9



Table 5: Mechanism for the copper ALD is divided into three parts: ligand exchange, reductive elimination and disproportionation. The various reaction energies are presented here for Zn compounds.

Reaction		Step	$\Delta E$ (kJ/mol)						
			L=acac	L=hfac	L=dmap	L=PyrIm <sup>R</sup> R= <sup>i</sup> Pr	L=PyrIm <sup>R</sup> R=Et	L=Cl	L=Et
Disproportionation	$\text{Zn}_2\text{L}_2 \rightarrow \text{Zn} + \text{ZnL}_2$	I	65.2	73.6	2.4	-83.3	-100.1	86.8	32.7
Ligand exchange for Zn(II)-Cu(II)	$\text{ZnL}_2 + \text{CuEt}_2 \rightarrow \text{LZnEt} + \text{LCuEt}$	II	-3.9	-14.9	2.6	-2.9	19.1	-21.2	
	$\text{LZnEt} + \text{LCuEt} \rightarrow \text{CuL}_2 + \text{ZnEt}_2$	III	4.7	-6.0	49.5	-0.3	18.9	34.9	
Ligand exchange for Zn(I)-Cu(II)	$\text{Zn}_2\text{L}_2 + \text{CuEt}_2 \rightarrow \text{LCuEt} + \text{Zn}_2\text{LEt}$	IV	140.7	119.7	-29.1	-110.0	-109.2	16.5	
	$\text{Zn}_2\text{LEt} + \text{LCuEt} \rightarrow \text{Zn}_2\text{Et}_2 + \text{CuL}_2$	V	-116.8	-87.8	-9.2	-23.3	-48.2	51.2	
Ligand exchange for Zn(II)-Zn(II)	$2\text{ZnLEt} \rightarrow \text{ZnL}_2 + \text{ZnEt}_2$	VI	-2.4	4.2	-3.9	-2.4	-26.7	35.8	
Reductive elimination	$2\text{LZnEt} \rightarrow \text{Zn}_2\text{L}_2 + \text{Et-Et}$	VII	-94.6	-96.4	-33.3	54.0	46.4	-78.0	-59.7
	$\text{LZnEt} \rightarrow \text{Zn} + \text{LEt}$	VIII	224.5	219.3	138.1	189.9	136.0	154.0	154.5
	$2\text{LZnEt} \rightarrow \text{Zn}_2\text{LEt} + \text{LEt}$	IX	303.9	280.3	104.0	166.1	107.7	105.4	-59.7
	$\text{Zn}_2\text{LEt} \rightarrow 2\text{Zn} + \text{LEt}$	X	145.1	158.2	172.1	213.8	164.3	203.6	203.6

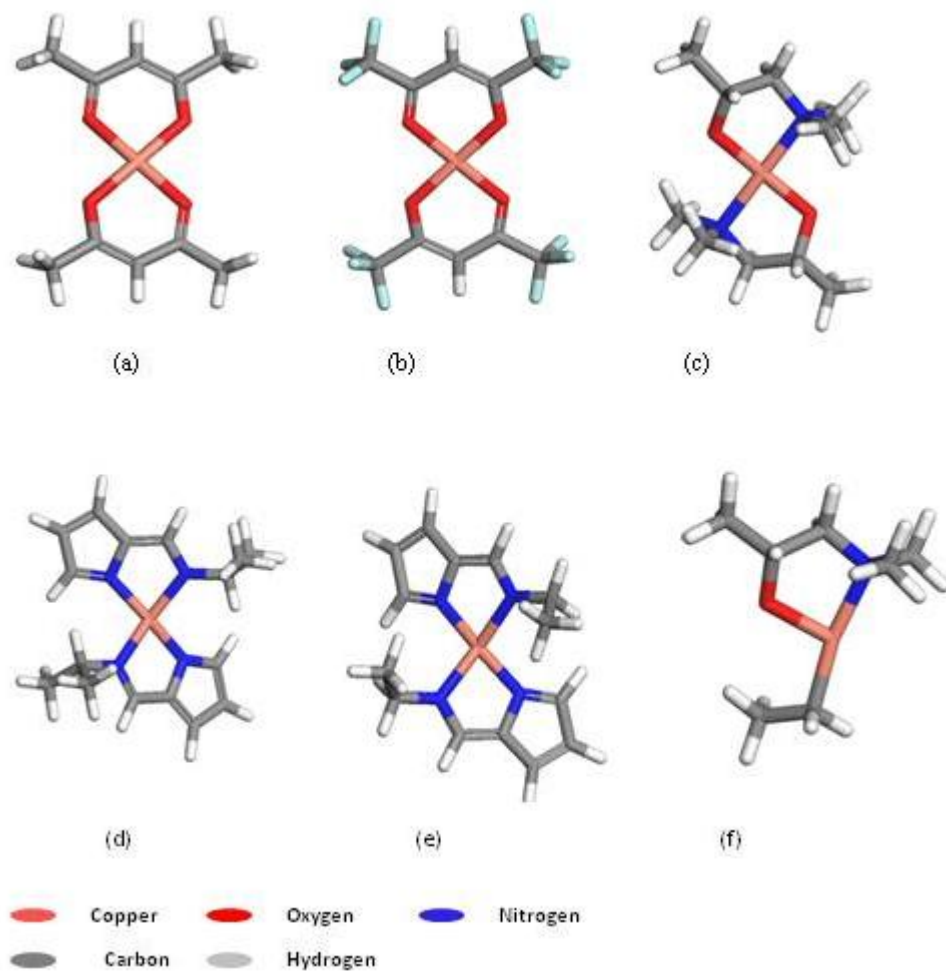


Figure 1 Stick representation of computed structures of precursors, intermediates and products. (a)  $\text{Cu}(\text{acac})_2$ , (b)  $\text{Cu}(\text{hfac})_2$ , (c)  $\text{Cu}(\text{dmap})_2$ , (d)  $\text{Cu}(\text{PyrIm}^{\text{iPr}})_2$ , (e)  $\text{Cu}(\text{PyrIm}^{\text{Et}})_2$  are the precursors used to understand the mechanism. (f)  $\text{Cu}(\text{dmap})\text{Et}$  is sample intermediate during the course of the reaction.

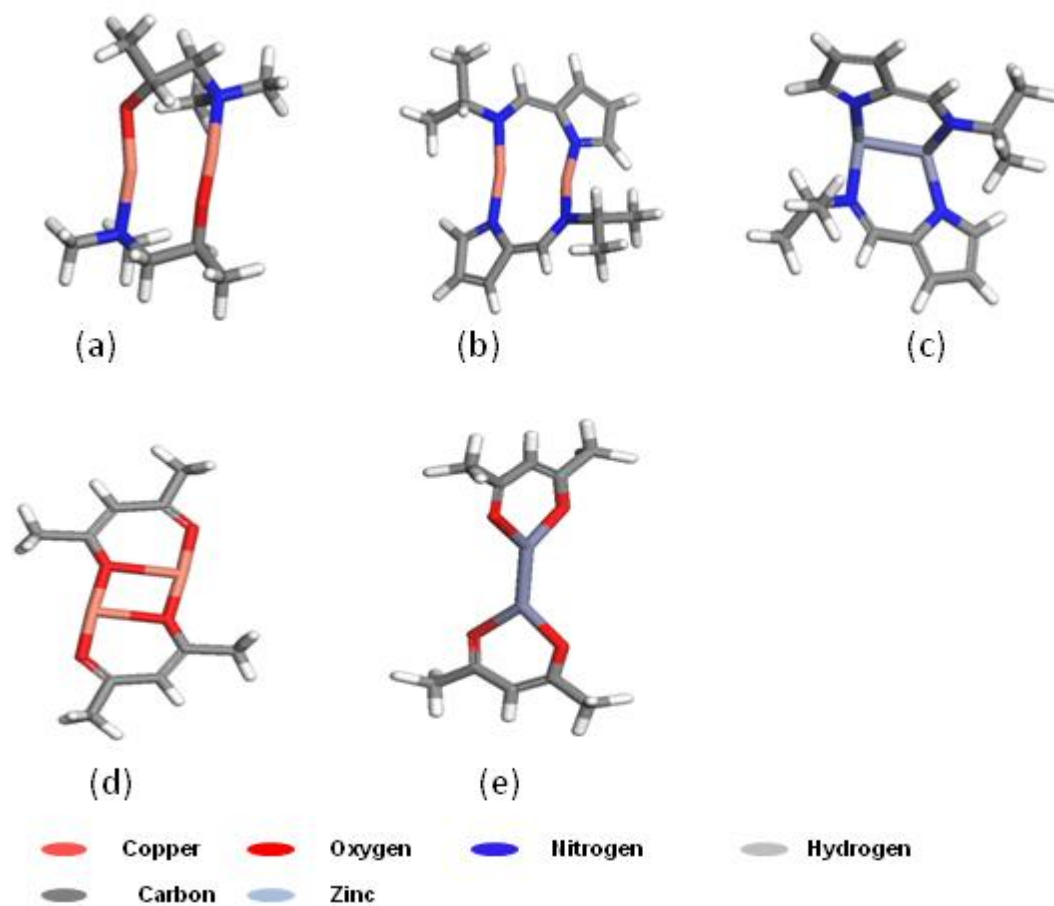


Figure 2 Stick representation of computed structures of intermediates of the type  $\text{Cu}_2\text{L}_2$ . (a)  $\text{Cu}_2(\text{dmap})_2$  (b)  $\text{Cu}_2(\text{PyrIm}^{\text{iPr}})_2$  and (c)  $\text{Zn}_2(\text{PyrIm}^{\text{iPr}})_2$  are nonplanar structures and (d)  $\text{Cu}_2(\text{acac})_2$  (e)  $\text{Zn}_2(\text{acac})_2$  are planar.

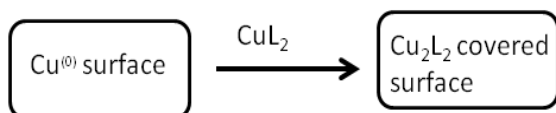
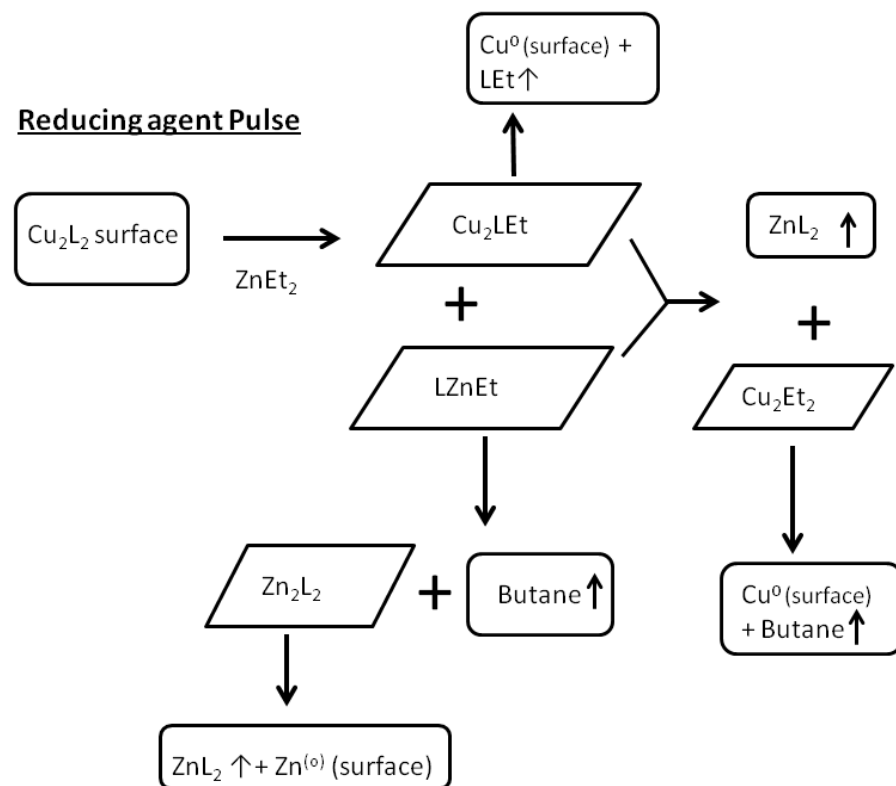
**Precursor Pulse****Reducing agent Pulse**

Figure 3 Flow chart to depict the possible ALD mechanism for both the precursor pulse and the reducing agent pulse. Rectangular shape denotes the starting reagents and the end products and slanted box denotes the intermediates. The upward arrow designates desorption of volatile species.